10th International Conference on Hydrodynamics
October 1-4, 2012 St. Petersburg, Russia

Propulsion and Steering Behaviour of a Ship Equipped with Two Contra-Rotating Z-drives

Manases Tello Ruiz[1], Guillaume Delefortrie[*2], Marc Vantorre[1], Stefan Geerts[1]
[1]Ghent University
Ghent, Belgium
[2]Flanders Hydraulics Research
Antwerp, Belgium
[*] E-mail: Guillaume.Delefortrie@mow.vlaanderen.be

ABSTRACT.

In 2011 captive manoeuvring tests have been carried out with a 1/25 scale model of an estuary vessel in the towing tank for manoeuvres in shallow water (co-operation Flanders Hydraulics Research – Ghent University). As this vessel was equipped with two contra-rotating Z-drives, a significant part of the testing program focussed on the propulsion and steering behaviour of this system, by repeating tests at different azimuth angles and propeller rates. These tests enabled the assessment of the interaction behaviour between the two drives and their effect on the propulsion and steering behaviour of the ship. In this way a mathematical model could be developed for implementation in a full mission inland ship manoeuvring simulator. The paper intends to give a description of the test-setup followed by an extensive discussion of the effect the Z-drives on the manoeuvring behaviour of the estuary vessel.

KEY WORDS: Contra-rotating Z-drives, azimuth thruster, thruster-thruster interaction, ship-thruster interaction.

INTRODUCTION

Azimuth drives are often applied for ships requiring higher manoeuvring capability, and are thus suitable for ships operating in confined waters. This is particularly the case for inland vessels, including those for fluvio-maritime service, called *estuary vessels* in this paper. Contra-rotating Z-drives are commonly accepted as the propulsion device giving the highest efficiency in several fields of marine industry and their efficiency has made them very attractive also for several types of DP-capable offshore vessels in the North Sea [1].

Vessel geometry, manoeuvring capabilities and power supply are main issues in the design of a propulsive system for estuary vessels. To meet these requirements more than one propulsion unit is used. This implies additional operational constraints related to thruster-thruster interaction such as blind azimuth angles and the propeller rates in overlap conditions. Such systems have mostly been implemented for dynamic DP systems and as a main propulsive unit for tugs which are constrained to operability ranges of low thruster advance numbers and flat bottom hull form shape. Different methods addressed to solve the hydrodynamic forces of azimuth drives can be found in the literature, based on experimental and theoretical researches [2-6], as well as on numerical methods [7].

Nienhuis [2] and Cozijn et al. [8] analysed the thruster effectiveness for azimuth drives for open water cases and mounted behind a flat barge. These scenarios were also studied by Stettler [4] with a ship hull form and a single propeller but no ship-thruster interaction was studied since the units were designed in a way the hull wake and boundary layer are outside the propeller slipstream.

The installation of azimuth drives in an estuary vessel requires more concern about the overall operability than in the case of thruster for DP systems and tugs. The manoeuvring requirements due to space restrictions imply the whole range of advance numbers and the hull form is different from a flat bottom barge, especially at the stern. The omni-directionality of the thruster units also requires some attention since it increases the probability of undesired ship-thruster or thruster-thruster interactions. Another important factor is the restriction of water depth for this type of vessels which might cause additional effects to the units.

To the authors' best knowledge, despite the work of Stettler [4], to date there is no literature concerning the influence of azimuth thrusters on the manoeuvring performance for estuary vessels. Thus, to investigate the manoeuvrability performance of an estuary vessel equipped with two contra-rotating azimuth drives, a series of captive manoeuvring tests has been carried out with a ship model in the towing tank for manoeuvres in shallow water (co-operation Flanders

Hydraulics Research – Ghent University) in Antwerp, Belgium.

EXPERIMENTAL SET UP

Model tests were carried out with a 1/25 scale model of the estuary container vessel *Tripoli*, operating between the coastal port of Zeebrugge and the hinterland via the Western Scheldt estuary, the main particulars of which are presented in Table 1. The ship is equipped with two Veth Z-drive rudder propellers, as presented in Table 2. Each azimuth propulsion drive is composed of two contra-rotating propellers; a pusher aft and a puller fore, the latter being ducted.

Table 1 Main particular of the estuary vessel.

Particular	Value	
L_{OA} (length over all)	110.0	m
L_{PP} (length between perpendiculars)	106.3	m
B (beam)	17.1	m
T (maximum draft)	4.5	m
D (depth)	5.7	m
∇ (volume displacement)	7140.0	m^3
C_B (block coefficient)	0.9	
x_G (longitudinal position centre of gravity)	-0.3	m
scale	1/25	

Table 2 Main particular of the counter-rotating Z-drives

Particular	Puller	Pusher
Propeller diameter	1.64 m	1.50 m
Design pitch ratio	1.02 m	1.13 m
Blade thickness	23 mm	21 mm
Expanded blade area ratio	0.7	0.9
Propeller rotation direction	Right handed	Left handed
Number of blades	4	5
Lateral distance between Z-drives	10.0 m	
Duct main characteristics		
Nozzle length	0.656 m	
Internal diameter	1.968 m	
External diameter	1.66 m	

The test program consisted of bollard pull, stationary, harmonic sway and yaw and multimodal tests; a description of the tests types can be found in [9-10]. The following parameters were varied: ship speed, drift angle, thruster rates and azimuth angles. Moreover, tests were also carried out at different under-keel-clearances and loading conditions (all even keel), see Table 3.

Table 3 Tested combinations of loading condition and gross under keel clearance (in % of draft)

4.50 m	3.78 m	2.52 m
150%	198%	346%
35%		
20%		
10%		

Coordinate systems and Conventions

Measurements of the thruster forces were performed in the ship bound longitudinal and transversal components, F_x and F_y (see Fig. 1(a)). The sign of the azimuth angle and the drift angle is shown in Fig. 1(b) and 1(c), respectively.

For convenience of the analysis of the thrusters units, the forces F_x and F_y were decomposed in the corresponding longitudinal and normal components T_{xp} and T_{yp}, respectively (see Fig. 1(a)), for the port side thrusters, and T_{xs} and T_{ys} for the starboard side thrusters.

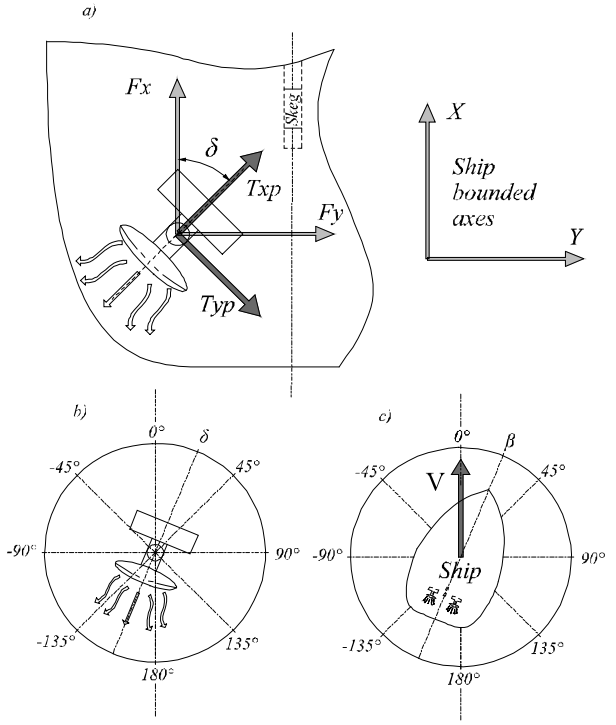

Fig. 1 Conventions for ship and thruster units.

In the present study the propellers' advance ratio, $J = \frac{V}{nD}$, is determined by the magnitude of the speed vector V and not by the apparent axial velocity. This is considered as large inflow angles are experienced by the units and using the axial inflow could lead to misunderstandings of the thrusters' performance. This was pointed out in [11] where the assumption of the apparent inflow velocity was only valid for small inflow angles or if the total advance ratio had a smaller value (see [3-5]).

DISCUSSION AND EXPERIMENTAL RESULTS

According to Stettler [4], the slipstream of the puller propeller strongly interacts with the pod housing and strut, producing pressure fluctuations and inclusive

large separation effects. This turns in an unsteady inflow to the pusher propeller.

Besides that, when more than one unit is installed, other parameters such as the location, disposition, rates of the thrusters and the complex astern hull form are main concerns of interaction between thruster-thruster and ship-thruster. For a propulsion unit installed at the ship its ambient flow is determined by the ship's wake being the first component of ship-thruster interaction. Moreover, due to the omni-directionality of the units, other sources of interaction might occur. For example, when the azimuth angle is $\delta = 180\,°$ the thrusters' slipstream is directed through the length of the ship, resulting in lower surface pressure and local friction losses [7], and for smaller azimuth angles, such as $\delta \approx 150\,°$ or $\delta \approx -150\,°$ for the starboard side and the portside units, respectively, the skeg of the ship might have an important effect on ship-thruster interaction.

While ship-thruster interaction is the result of the installation of the units, thruster-thruster interaction is a consequence of the omni-directionality of the thrusters. A large number of configurations of the thrusters is possible, which could lead to scenarios where one of the units (trailing thruster) is operating in ambient flow partially or totally influenced by the slipstream of the other one (leading thruster). Fig. 2 shows some arrangements where thruster-thruster interaction occurs for the portside unit.

To better understand the thruster forces developments, the experimental data is presented in two sections: thruster forces at bollard pull condition and thruster forces with nonzero ship velocity.

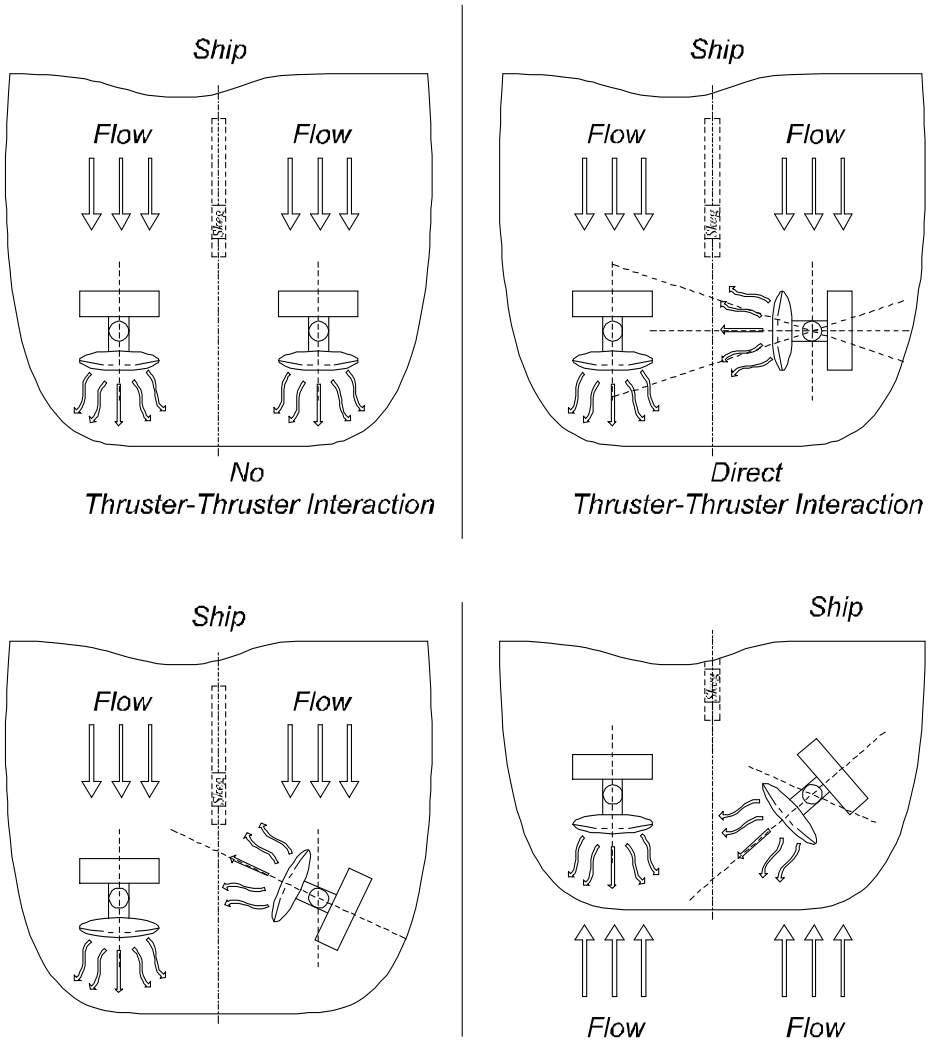

Fig. 2 Scenarios of thruster-thruster interaction

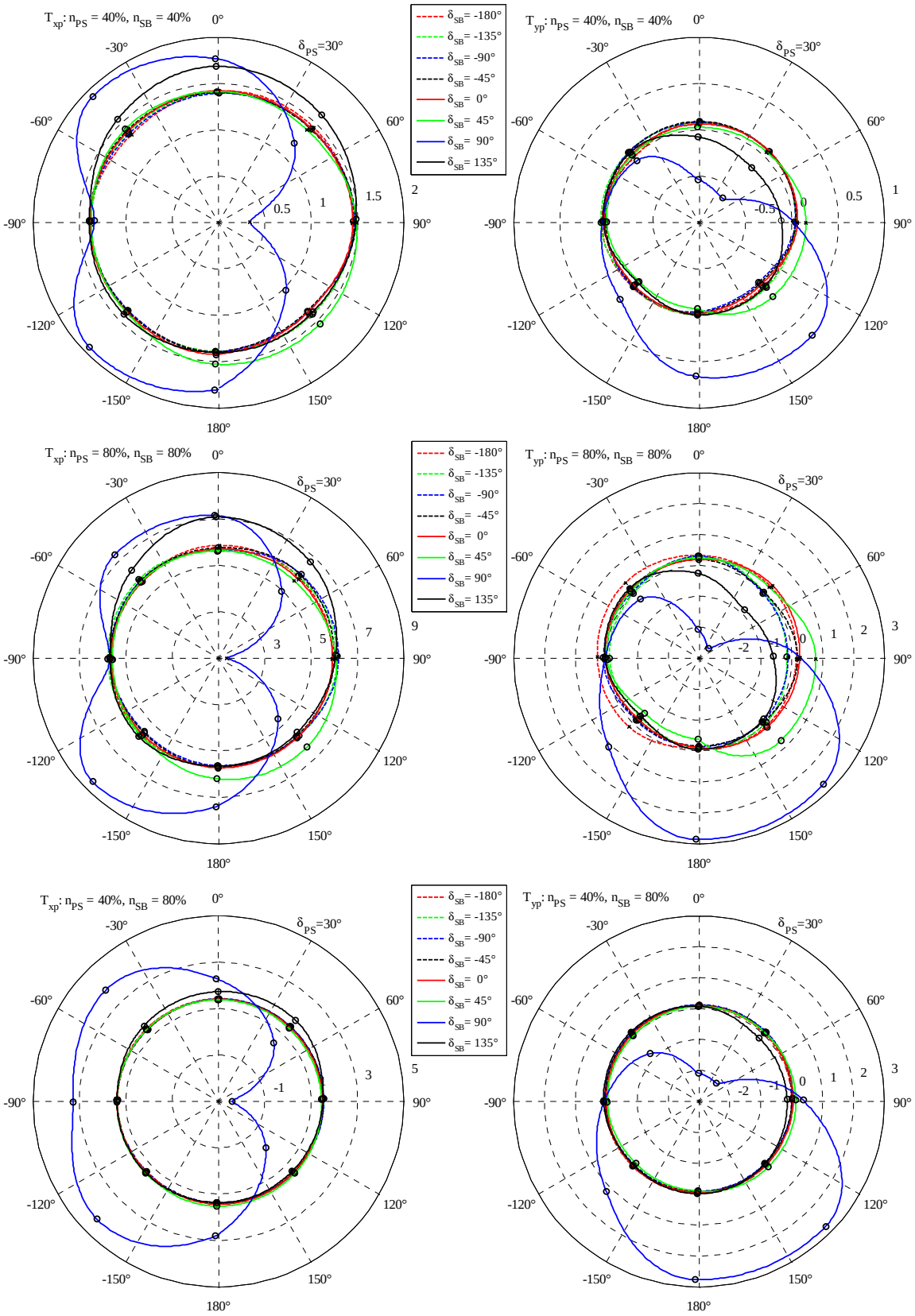

Fig. 3 $T_{xp}(a, c, e)$ (left column) and $T_{yp}(b, d, f)$ (right column) for the portside unit at bollard pull conditions for the fully loaded vessel at 150% under keel clearance
(a),(b) $n_{PS} = 40\%$ and $n_{SB} = 40\%$
(c),(d) $n_{PS} = 80\%$ and $n_{SB} = 80\%$
(e),(f) $n_{PS} = 40\%$ and $n_{SB} = 80\%$
The legends refer to azimuth angles δ_{SB} of the starboard thruster.

Thruster Forces Development at Bollard Pull

General Observations. Bollard pull tests are carried out with zero speed and zero acceleration; therefore, the thruster rates, n_{SB} and n_{PS}, and the azimuthal angles, δ_{SB} and δ_{PS}, are the only parameters in this analysis. Fig. 3 presents the plots of the thrust force, T_{xp}, and the normal force, T_{yp}, for the portside unit at bollard pull condition while the fully loaded ship has an under keel clearance of 150% of the draft. In the plots the markers represent the measured values and the lines their interpolation.

In Fig. 3 the arrangement is as follows: the first column (a, c, e) and the second column (b, d, f) are plots of T_{xp} and T_{yp}, respectively, and the rows are arranged for the same set of propeller rates. For each polar plot the presented results correspond to a fixed position of the azimuth angle of the starboard side unit while the azimuthal angle of the portside unit varies between $\delta_{PS} = 0°$ and $\delta_{PS} = 360°$, either in clockwise or counter-clockwise direction.

Observing Fig. 3 (a, b), two main zones can be determined based on the forces, generated by the portside unit in T_{xp} and T_{yp}, corresponding to azimuthal positions of the starboard side unit. The first zone is determined by direct interaction where the portside unit operates in ambient flow determined by the slipstream of the starboard side thruster; this corresponds to azimuthal configurations of the starboard side unit varying between $\delta_{SB} = 45°$ to $135°$. The second zone covers all other angles where insignificant fluctuation of T_{xp} and T_{yp} is observed.

Thrust force. For the thrust force generated by the port side thruster (see Fig.3 (a)) while the starboard side unit has an azimuth angle of $\delta_{SB} = 90°$, three zones with positive, negative and zero interaction effects can be observed, corresponding with increasing, decreasing and unchanging thrust force, respectively.

For azimuthal angles of the portside unit between $\delta_{PS} \approx 20°$ and $160°$ the net inflow velocity is increased due to the slipstream of the starboard side unit. This decreases the effective angle of attack and, consequently, the thrust force. This effect reaches a maximum as the portside unit reaches the azimuthal position of $\delta_{PS} = 90°$ where it is aligned with the slipstream of the starboard unit.

The opposite effect occurs for the remaining sector of azimuthal angles ($\delta_{PS} < 20°$ or $\delta_{PS} > 160°$). In this scenario the inflow velocity is negative, thus increasing the angle of attack of the propeller blades and, hence, the thrust force. However, in this range of azimuthal angles of the portside unit a cancellation of the interaction effects is found for $\delta_{PS} = -90°$. This seems to be logical since both thrusters are operating at the same rate and are arranged in opposite direction. As a result, the slipstream velocities developed by both units are equal but in opposite directions, i.e. leading to zero inflow velocity and, therefore, no thrust force variation.

A strengthening of the interaction effects to the thrust force can be observed in Fig. 3 (c, e) where the rate of both propulsion units has increased to $n_{SB} = n_{PS} = 80\%$ of the maximum rpm. However, similar to Fig. 3(a), Fig. 3(c) also experiences the zero interaction zone for $\delta_{PS} = -90°$ confirming that an equivalent zero inflow velocity to the portside unit occurs for configurations where the rates of both thrusters are set to the same value. This can be clearly seen when observing Fig. 3(e) where the propeller rates of the thrusters are different, which largely affects the thrust produced by the portside unit at $\delta_{PS} = -90°$.

Normal force. The normal force (see Fig. 3 (b)) is a result of a complex combination of effects such as the lift and drag of the blades, the strut and the duct. Since the rate of the thrusters is held constant (for each polar plot) and the velocities and acceleration are set to zero, the ambient flow will be determined by the slipstream of the starboard side unit for the zones where interaction takes place. Thus, the variation of T_{yp} of the portside unit will only be dependent of its own propeller rate and the slipstream of the starboard side unit.

As observed for T_{xp} in Fig. 3(a), the variation of T_{yp} (see Fig. 3(b)) is drastically influenced for azimuthal positions of the starboard side unit varying from $\delta_{SB} = 45°$ to $135°$, with a stronger interaction at $\delta_{SB} = 90°$. When the azimuth angle of the starboard side unit varies within that range, the portside unit experiences larger interaction effects for almost every azimuthal position.

When comparing T_{yp} from Fig. 3(d) and Fig. 3 (f) for configurations where stronger thruster-thruster interaction occurs, one can see the value of T_{yp} does not vary significantly when the rate of the portside unit is changed. Thus, it can be stated that in the presence of the stronger thruster-thruster interaction the own contribution of the portside unit to its normal force is rather small. On the other hand for $\delta_{SB} = 45°$ to $135°$, a contribution of the own rate of the portside unit is observed to T_{yp}; however, it is only significant at higher rates of the portside unit.

Thruster forces developed with nonzero ship speed

Thrust force. Fig. 4 presents the results of the thrust coefficient, K_{Txp}, for the portside unit evaluated at different combinations of advance number, J, and drift angle, β, while both thrusters are set to zero azimuth angle. In Fig. 4 the plotted results in the top and the bottom correspond to an under keel clearance of 150% and 35% respectively.

It is important to remember that, as mentioned before, $J = \frac{V}{nD}$ is based on the magnitude of the total ship velocity vector V, instead of the axial velocity component relative to the thrust unit as in [4].

In Fig. 4 (a), it can be seen that the values of K_{Txp} are approximately the same for small drift angles varying from $\beta = -10°$ to 10°, and they diverge more from each other as β increases. Additionally, some differences between K_{Txp} for positive and negative drift angles are observed; these differences appear to be important for $\beta = 60°$ and $-60°$, but nearly non-existent for $\beta = 90°$ and $-90°$.

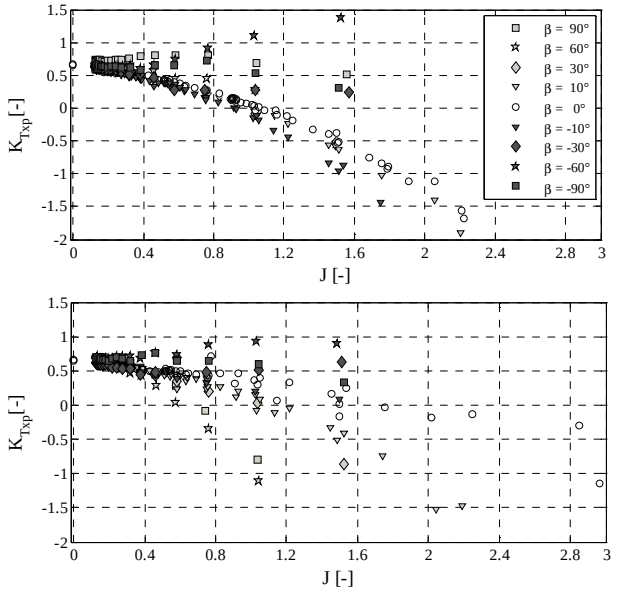

Fig. 4 K_{Txp} for the portside unit at: (a) $ukc = 150\%$ (above) and (b) $ukc = 35\%$ (below). The azimuth angle of both thrusters was set to $\delta_{SB} = \delta_{PS} = 0°$

These differences in K_{Txp} for negative and positive drift angles can be explained by the interaction between the thrust unit and the ship. This seems to be confirmed when looking to drift angles of $\beta = 60°$ and $\beta = -60°$ where the values corresponding to the negative drift result into higher K_{Txp} values compared to the corresponding positive angle. From Fig. 2, it can be seen that the skeg of the ship interferes with the free inflow in case of negative drift angles; the flow pattern is deviated in such a way that the portside unit is subjected to a condition similar to bollard pull.

The first observation seems to be logical since a small variation in the inflow angle (in this case β) does not change significantly the net inflow velocity to propeller disc, thus the effective angle of attack to the propeller blades and, hence, the thrust force, remain approximately equal. However, when the inflow angle is larger, the net axial inflow velocity to the propeller is also reduced thus the development of K_{Txp} is closer to the bollard pull value. In fact it is expected that for $\beta = 90°$ and $\beta = -90°$ the thrust should be constant and equal to the bollard pull case, however this is not observed. This can be attributed to an angular deviation of the flow in the vicinity of the thruster unit, resulting in a non-zero inflow velocity into the propeller blades.

Other important issues can be pointed out when comparing the results of $ukc = 150\%$ with the ones relative to $ukc = 35\%$. The complex wake field as a result of the decrease of the water depth causes more scatter of K_{Txp}. In general, an increase of the thrust is observed, e.g. when comparing the curves of K_{Txp} for $\beta = 0°$; the deep water curve is significantly steeper than the curve for $ukc = 35\%$.

Fig. 5 presents the results of K_{Txp}, of the portside thruster for a discrete number of J values while the ship is moving ahead with $\beta = 0°$ and both units are operating in tandem condition ($\delta_{SB} = \delta_{PS}$) for a variation of azimuth angles covering 360°. In Fig. 5 the top and the bottom figures correspond to $ukc = 150\%$ and $ukc = 35\%$ respectively.

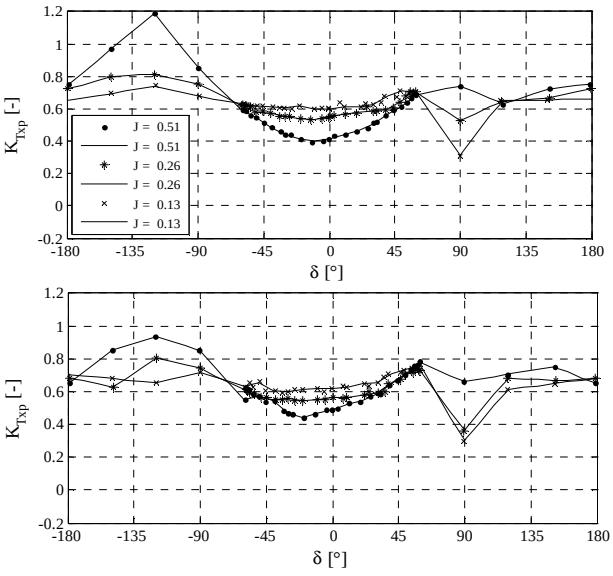

Fig. 5 K_{Txp} for the portside unit at: (a) ukc $= 150\%$ (above) and (b) ukc $= 35\%$(below). Both units operate in tandem condition ($\delta_{SB} = \delta_{PS}$) at zero drift angle $\beta = 0°$.

The variation of K_{Txp} for a constant advance ratio J defines zones of operation for the thrust force. Looking to Fig. 5(a), four zones can be identified corresponding to azimuth angles:

- $\delta = -180° \; to \; \delta \approx -60°$;
- $\delta \approx -60° \; to \; \delta \approx 60°$;
- $\delta \approx 60° to \; \delta \approx 120°$;
- $\delta \approx 120° \; to \; \delta = 180°$.

The development of the thrust force shows higher K_{Txp} values in the first zone, $\delta = -180° \; to \; \delta \approx -60°$. This increase in K_{Txp} is mainly related to the negative inflow velocity to the thruster. Thus, one could expect higher K_{Txp} values for $\delta = -180°$ when compared to $\delta = 120°$, as the inflow velocity decreases with the increase in the inflow angle. However, this is not observed and the opposite holds true. In fact, when $\delta = -180°$, the thrust coefficient takes a value of K_{Txp} which is closer to the bollard pull value. This might indicate that the velocity in the slipstream of the other thruster is strong enough to cancel the wake of the ship at those advance numbers. The higher values for $\delta = -120°$ can be addressed to the fact that at this azimuthal positions part of the thruster slipstream is turned off by the stern of the ship, thus reinforcing the inflow velocity and consequently increasing the effective blade angle of attack and, hence, the thrust force.

When the azimuth angle is set between $\delta = -60°$ to $60°$ the inflow velocity to the thruster is positive, thus a decrease in the thrust force is expected at larger J numbers or smaller δ angles, e.g. the lowest value of K_{Txp} is experienced at $\delta = 0°$.

Some important observation can be made when looking to the range of azimuth angles between $\delta = 60°$ to $180°$. An important drop of the magnitude is experienced at $\delta = 90°$, which corresponds to the scenario of direct interaction. However, this effect is less pronounced for larger J numbers suggesting that the slipstream of the starboardside unit is deviated from the location of the portside unit, e.g. the lowest drop of K_{Txp} corresponds to the advance number $J = 0.51$ keeping its tendency with respect to previous azimuthal positions.

However, when the azimuth angle of the thrust units are set to higher values than $\delta = 90°$, K_{Txp} seems to be subjected to a zero ambient flow. This, as discussed for $\delta = -180°$, would mean a cancelation of the wake of the ship. This can be understood as the indirect interaction effects between the thrusters units. When they are set to this range of azimuthal positions the slipstream of the starboard side unit is directed opposite to the approaching flow (wake of the ship) of the portside unit thus decreasing the effect of the wake of the ship and turning the ambient flow to a similar case as the bollard pull.

The results of K_{Txp} obtained for $ukc = 35\%$ generally follow the same pattern described for $ukc = 150\%$. However, the shallow water curves varies less drastically as the ones of deep water. This seems to be the most important effect when the under keel clearance is reduced as observed when the influence of the drift angle was discussed.

Normal force. The normal force to the thruster units at a constant ship speed with both thrusters at $\delta = 0°$, is presented in Fig. 6 where the results are plotted as a function of the ratio between the rate of the propellers, n, and the maximum rate, n_0, for different drift angles. The results are presented for two different water depths.

At $ukc = 150\%$ T_{YP} increases for positive drift angles and varies around $T_{YP} = 0(N)$ for negative ones. This was also observed for K_{Txp} (see Fig. 4), indicating that for negative drift angles the ambient velocity at the vicinity of the portside unit is partially deviated by the ship hull and the skeg, thus resulting small T_{YP} forces.

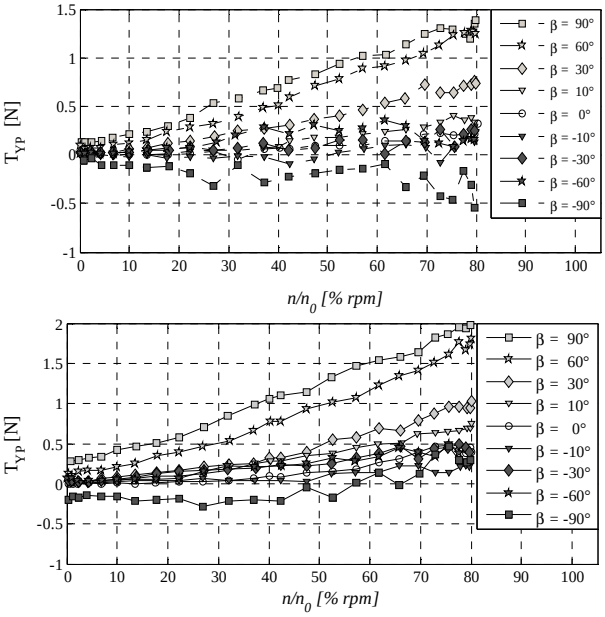

Fig. 6 T_{YP} for the portside thruster unit at $\delta = 0°$ and ship speed $V = 0.18\, m/s$ (model scale). (a) $ukc = 150\%$ (above) and (b) $ukc = 35\%$ (below).

Additionally to the increase for positive drift angles, it is also observed that T_{YP} increases approximately linearly with the rate of the thruster unit reaching values higher than 0.5N even for low propeller rates.

Although the environmental conditions of the thruster units at sailing and bollard pull condition are different, comparing the magnitude of T_{YP} some conclusion can be drawn. The large values of T_{YP} observed at Fig. 6(a) for smaller propeller rates seems to be contradictory to what have been observed at bollard pull condition (see Fig. 3 (b, f).

However, when comparing T_{YP} from Fig. 6(a) and Fig. 3 (b, f) it is observed a significant difference. The maximum values of T_{YP} reached for the bollard pull condition show higher magnitudes than the ones in Fig. 6(a), meaning that the ambient velocity experienced in Fig. 3 (b, f) is stronger than the one in Fig. 6(a). This strong ambient velocity could explain why in Fig. 3 (b, f) there was no significant values of T_{YP} for lower rates of the own portside unit.

The same behaviour described for $ukc = 150\%$ is observed for $ukc = 35\%$. However, in the latter case, T_{YP} presents higher values and a more uniform tendency to $T_{YP} = 0\ N$ for negative β. The values of T_{YP} at $n/n_0 = 0$ confirm this relative strengthening of the effect of the velocity but only for drift angles higher than $\beta >= 30°$. This could be explained by the increasing $2D$ behaviour of the flow as the ukc is decreased.

CONCLUSIONS

Azimuth thrusters possibly offer large advantages in manoeuvring, but the understanding of the hydrodynamic phenomena are important in their design stage to avoid larger thrust degradation and unwanted ship forces.

The results of the present study clearly show the interaction effect between the thruster units and the interaction between the ship and the thruster, identifying defined zones where a contribution of the slipstream of the unaffected thruster to the ambient flow of the affected unit is considerable and zones where the skeg of the ship diverge away the ambient flow thus generating large wake factors. Moreover, both a reduction and an increment of those effects can be found for smaller under keel clearances.

ACKNOWLEDGEMENTS

This research was funded by the department of Mobility and Public Works of the Flemish Government, Belgium. The authors wish to thank Veth Propulsion, The Netherlands, for their willingness to share the plans of their Z-drives and GSP Projects, Belgium, for sharing the line plans of the estuary vessel MS Tripoli.

REFERENCES

[1] Jukola H. Thrusters Contra-Rotating Propellers – Combination of DP Capability, Fuel Economy and Environment. Dynamic Positioning Conference, Houston , USA, October 17-18, 2006 .

[2] Nienhuis U. Analysis of Thruster effectivity for dynamic Positioning and Low Speed Manoeuvring, PhD Thesis, Delft University of Technology, 1982.

[3] Bradner P. and Renilson, M., Interaction Between Two Closely Spaced Azimuthing Thrusters. Journal of Ship Research, Vol. 42, No. 1, March 1998.

[4] Stettler J. Steady and Unsteady Dynamics of an Azimuthing Podded Propulsor Related to Vehicle Maneuvering, PhD Thesis, Massachusetts Institute of Technology, 2004.

[5] Islam M.F., Veitch B., and Liu P. Experimental Research on Marine Podded Propulsor. Journal of Naval Architecture and Marine Engineering, vol. 4, no. 2, pp. 57-71, Sep. 2008.

[6] Amini H., and Steen S. Experimental and Theoretical Analysis of Propeller Shaft Loads in Oblique Inflow, Journal of Ship Research, vol. 55, pp. 267-288, 2011.

[7] Dang J. and Laheij H. Hydrodynamic Aspects of Steerable Thrusters. Dynamic Positioning Conference, Houston , USA, September 28-30, 2003

[8] Cozijn H., Hallmann R. and Koop A. Analysis of the Velocities in the Wake of an Azimuthing Thruster, using PIV Measurements and CFD Calculations. Dynamic Positioning Conference, Houston, USA, October 12-13, 2010

[9] Delefortrie G. Manoeuvring Behaviour of Container Vessels in Muddy Navigation Areas, PhD Thesis, Gent University, 2009.

[10] K. Eloot. Selection, Experimental Determination and Evaluation of a Mathematical Model for Ship Manoeuvring in Shallow Water, PhD thesis, Ghent University, 2006.

[11] Oosterveld M.W.C and Oortmerssen G. Thruster Systems for Improving the Maneuverability And Position-Keeping Capability of Floating Objects. Offshore Technology Conference, Texas, USA, 1972.